Exploring Phase Transitions in the Two Dimensional Ising Model

Cory Alexander Balaton & Janita Ovidie Sandtrøen Willumsen
https://github.uio.no/FYS3150-G2-2023/Project-4
(Dated: May 31, 2024)

We have studied the ferromagnetic behavior of the Ising model at a critical temperature, when undergoing phase transition. To generate spin configurations, we used the Metropolis-Hastings algorithm, which applies a Markov chain Monte Carlo sampling method. We determined the time of equilibrium to be approximately 5000 Monte Carlo cycles, and used the following samples to find the probability distribution at temperature $T_1 = 1.0J/k_B$, and $T_2 = 2.4J/k_B$. For T_1 the mean energy per spin is $\langle\epsilon\rangle \approx -1.9972J$, with a variance $\mathrm{Var}(\epsilon) = 0.0001$. And for T_2, close to the critical temperature, the mean energy per spin is $\langle\epsilon\rangle \approx -1.2367J$, with a variance $\mathrm{Var}(\epsilon) = 0.0202$. In addition, we estimated the expected energy and magnetization per spin, the heat capacity and magnetic susceptibility. We have estimated the critical temperatures of finite lattice sizes, and used these values to approximate the critical temperature of a lattice of infinite size. Using linear regression, we estimated the critical temperature to be $T_c^*(L = \infty) \approx 2.2693J/k_B$.

I. INTRODUCTION

Magnetic materials are used in a variety of technological devices. The distinct magnetic property of these materials is utilized in devices such as compasses for navigation, in computer hard drives to store data [1], and MRI machines to produce detailed anatomical images.

Magnetic materials care classified based on their specific magnetic behavior, and one of the groups consists of ferromagnetic materials. These materials are easily magnetized, and when exposed to a strong magnetic field, they become saturated. In addition, when these materials are heated to a critical point, they lose their magnetic property [2].

The Ising model was introduced by Wilhelm Lenz and Ernst Ising in the early 1920s, in an attempt to simulate a physical system of ferromagnets using statistical mechanics [3]. The model have later been used to describe other phenomena, such as networks of neurons [4].

We will use the Ising model to study the behavior in ferromagnets when they are exposed to temperatures near a critical point. In addition, we will numerically estimate the critical temperature where the system experience phase transition.

In Section II, we will present the theoretical background for this experiment, as well as the algorithms and tools used in the implementation. Continuing with Section III, we will present our results and discuss our findings. Lastly, we will conclude our findings in Section IV.

II. METHODS

A. The Ising model

The Ising model consists of a lattice of spins, which can be thought of as atoms in a grid. In two dimensions, the length of a lattice is given by L, and the number of spins within a lattice is given by $N = L^2$. When we consider the entire lattice, the system spin configuration is represented as a matrix $L \times L$

$$\mathbf{s} = \begin{pmatrix} s_{1,1} & s_{1,2} & \cdots & s_{1,L} \\ s_{2,1} & s_{2,2} & \cdots & s_{2,L} \\ \vdots & \vdots & \ddots & \vdots \\ s_{L,1} & s_{L,2} & \cdots & s_{L,L} \end{pmatrix} .$$

The total number of possible spin configurations, also called microstates, is $|\mathbf{s}| = 2^N$.

A given spin i can take one of two possible discrete values $s_i \in \{-1, +1\}$. The spins interact with its nearest neighbors, and in a two-dimensional lattice each spin has up to four nearest neighbors. In our experiments we will use periodic boundary conditions, resulting in all spins having exactly four nearest neighbors. To find the analytical expressions necessary for validating our model implementation, we assume a 2×2 lattice.

The hamiltonian of the Ising model is given by

$$E(\mathbf{s}) = -J \sum_{\langle kl \rangle}^{N} s_k s_l - B \sum_{k}^{N} s_k \ , \tag{1}$$

where $\langle kl \rangle$ denotes a spin pair. J is the coupling constant, and B is the external magnetic field. For simplicity, we consider the Ising model where $B = 0$, and find the total system energy given by

$$E(\mathbf{s}) = -J \sum_{\langle kl \rangle}^{N} s_k s_l \ . \tag{2}$$

We count the neighboring spins using the pattern visualized in Figure 1, to avoid counting a given spin pair several times. We also find the total magnetization of the system, which is given by

$$M(\mathbf{s}) = \sum_{i}^{N} s_i \ . \tag{3}$$

In addition, we have to consider the state degeneracy, the number of different microstates sharing the same value of

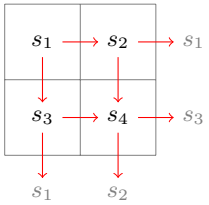

FIG. 1: Visualization of counting rules for each pair of spins in a 2×2 lattice, where periodic boundary conditions are applied.

total magnetization. In the case where we have two spins oriented up, the total energy have two possible values, as shown in Appendix A.

Spins up	$E(\mathbf{s})$	$M(\mathbf{s})$	Degeneracy
4	-8J	4	1
3	0	2	4
2	0	0	4
	8J	0	2
1	0	-2	4
0	-8J	-4	1

TABLE I: Values of the total energy, total magnetization, and degeneracy for the possible states of a system for a 2×2 lattice, with periodic boundary conditions.

We calculate the analytical values for a 2×2 lattice, found in Table I. However, we scale the total energy and total magnetization by the number of spins, to compare these quantities for lattices where $L > 2$. Energy per spin is given by

$$\epsilon(\mathbf{s}) = \frac{E(\mathbf{s})}{N} \ , \tag{4}$$

and magnetization per spin given by

$$m(\mathbf{s}) = \frac{M(\mathbf{s})}{N} \ . \tag{5}$$

B. Statistical mechanics

When we study the behavior of the Ising model, we have to consider the probability of a microstate $\mathbf{s}$ at a fixed temperature T. The probability distribution function (pdf) is given by

$$p(\mathbf{s} \mid T) = \frac{1}{Z} \exp^{-\beta E(\mathbf{s})}, \tag{6}$$

known as the Boltzmann distribution. This is an exponential distribution, where β is given by

$$\beta = \frac{1}{k_B} \ , \tag{7}$$

where and k_B is the Boltzmann constant. Z is a normalizing factor of the pdf, given by

$$Z = \sum_{\text{all possible } \mathbf{s}} e^{-\beta E(\mathbf{s})} \ , \tag{8}$$

and is known as the partition function. We derive Z in Appendix B, which gives us

$$Z = 4\cosh(8\beta J) + 12 \ .$$

Using the partition function and Equation (6), the probability of a microstate at a fixed temperature is given by

$$p(\mathbf{s} \mid T) = \frac{1}{4\cosh(8\beta J) + 12} e^{-\beta E(\mathbf{s})} \ . \tag{9}$$

We find the expected total energy

$$\langle E \rangle = -\frac{8J\sinh(8\beta J)}{\cosh(8\beta J) + 3} \ , \tag{10}$$

and the expected energy per spin

$$\langle \epsilon \rangle = \frac{-2J\sinh(8\beta J)}{\cosh(8\beta J) + 3} \ . \tag{11}$$

We find the expected absolute total magnetization

$$\langle |M| \rangle = \frac{2(e^{8\beta J} + 2)}{\cosh(8\beta J) + 3} \ , \tag{12}$$

and the expected magnetization per spin

$$\langle |m| \rangle = \frac{e^{8\beta J} + 1}{2(\cosh(8\beta J) + 3)} \ . \tag{13}$$

We derive the analytical expressions for expectation values in Appendix C.

We also need to determine the heat capacity

$$C_V = \frac{1}{k_B T^2}(\mathbb{E}(E^2) - [\mathbb{E}(E)]^2) \ , \tag{14}$$

and the magnetic susceptibility

$$\chi = \frac{1}{k_{\mathrm{B}T}}(\mathbb{E}(M^2) - [\mathbb{E}(M)]^2) \ . \tag{15}$$

In Appendix D we derive expressions for the heat capacity and the susceptibility, and find the heat capacity

$$\frac{C_V}{N} = \frac{64J^2}{Nk_BT^2}\left(\frac{3\cosh(8\beta J) + 1}{(\cosh(8\beta J) + 3)^2}\right) \ ,$$

and magnetic susceptibility

$$\frac{\chi}{N} = \frac{4}{Nk_BT}\left(\frac{3e^{8\beta J} + e^{-8\beta J} + 3}{(\cosh(8\beta J) + 3)^2}\right) \ .$$

For scalability of our model, we want to work with unitless spins. To obtain this, we introduce the coupling

constant J as the base unit for energy. With the Boltzmann constant we derive the remaining units, which can be found in Table II.

Value	Unit	
$[E]$	J	
$[M]$	1	(unitless)
$[T]$	J/k_B	
$[C_V]$	k_B	
$[\chi]$	$1/J$	

TABLE II: Values of the total energy, total magnetization, and degeneracy for the possible states of a system for a 2×2 lattice, with periodic boundary conditions.

C. Phase transition and critical temperature

We consider the Ising model in two dimensions, with no external external magnetic field. At temperatures below the critical temperature T_c, the Ising model will magnetize spontaneously. When increasing the temperature of the external field, the Ising model transitions from an ordered to an unordered phase. The spins become more correlated, and we can measure the discontinuous behavior as an increase in correlation length $\xi(T)$ [5, p. 432]. At T_c, the correlation length is proportional to the lattice size, resulting in the critical temperature scaling relation

$$T_c(L) - T_c(L = \infty) = aL^{-1} \ , \tag{16}$$

where a is a constant. For the Ising model in two dimensions, with a lattice of infinite size, the analytical solution of the critical temperature is

$$T_c(L = \infty) = \frac{2}{\ln\left(1 + \sqrt{2}\right)} J/k_B \approx 2.269 J/k_B \tag{17}$$

This result was found analytically by Lars Onsager in 1944 [6]. We can estimate the critical temperature of an infinite lattice, using the critical temperature of finite lattices of different sizes and linear regression.

D. The Markov chain Monte Carlo method

Markov chains consist of a sequence of samples, where the probability of the next sample depends on the probability of the current sample. Whereas the Monte Carlo method introduces randomness to the sampling, which allows us to approximate statistical quantities [7] without using the pdf directly. We generate samples of spin configuration, to approximate $\langle \epsilon \rangle$, $\langle |m| \rangle$, C_V, and χ, using the Markov chain Monte Carlo (MCMC) method.

The Ising model is initialized in a random state, and the Markov chain is evolved until the model reaches an equilibrium state. However, generating new random states requires ergodicity and detailed balance. A Markov chain is ergoditic when all system states can be reached at every current state, whereas detailed balance implies no net flux of probability. To satisfy these criteria we use the Metropolis-Hastings algorithm, found in Algorithm 1, to generate samples of microstates.

One Monte Carlo cycle consists of N attempted spin flips. When a spin is flipped, the change in energy is evaluated as

$$\Delta E = E_{\text{after}} - E_{\text{before}} \ ,$$

and accepted if $\Delta E \leq 0$. However, if $\Delta E > 0$ we have to compute the Boltzmann factor

$$p(\mathbf{s}|T) = e^{-\beta \Delta E} \tag{18}$$

Since the total system energy only takes three different values, the change in energy can take 3^2 values. However, there are only five distinct values $\Delta E = \{-16J, -8J, 0, 8J, 16J\}$, we derive these values in Appendix E. We can avoid computing the Boltzmann factor, by using a look up table (LUT). We use ΔE as an index to access the resulting value of the exponential function, in an array.

Algorithm 1 Metropolis-Hastings Algorithm

procedure METROPOLIS($lattice, energy, magnetization$)
  for Each spin in the lattice **do**
    $ri \leftarrow$ random index of the lattice
    $rj \leftarrow$ random index of the lattice
    $dE \leftarrow 2 \cdot lattice_{ri,rj} \cdot (lattice_{ri,rj-1} + lattice_{ri,rj+1} + lattice_{ri-1,rj} + lattice_{ri+1,rj})$
    $rn \leftarrow$ random number $\in [0, 1)$
    if $rn \leq e^{-\frac{dE}{T}}$ **then**
      $lattice_{ri,rj} = -1 \cdot lattice_{ri,rj}$
      $magnetization = magnetization + 2 \cdot lattice_{ri,rj}$
      $energy = energy + dE$

The Markov process reaches an equilibrium after a certain number of Monte Carlo cycles, called burn-in time. After the burn-in time, the system state reflects the state of a real system, and we can start sampling microstates. The probability distribution of the samples will tend toward the actual probability distribution of the system.

E. Implementation and testing

We implemented a test suite, and compared the numerical estimates to the analytical results from Section II B. In addition, we set a tolerance to verify convergence, and a maximum number of Monte Carlo cycles to avoid potentially having the program run indefinitely.

We used a pattern to access all neighboring spins, where all indices of the neighboring spins are put in an $L \times 2$ matrix. The indices are accessed using pre-defined constants, where the first column contain the indices for neighbors to the left and up, and the second column right and down. This method avoids the use of if-tests, so we can take advantage of the compiler optimization.

We parallelized our code using both message passing interface (OpenMPI) and multi-threading (OpenMP). First, we divided the temperatures into smaller sub-ranges, and each MPI process received a sub-range of temperatures. Every MPI initialize a parallel region with a set of threads, which then initializes an Ising model and performs the Metropolis-Hastings algorithm. We limited the number of times threads are spawned and joined, by using single parallel regions, reducing parallel overhead. We used Fox [1], a high-performance computing cluster, to run our program for 1 and 10 million Monte Carlo cycles when analyzing phase transitions.

F. Tools

The Ising model and MCMC methods are implemented in C++, and parallelized using both `OpenMPI` [8] and `OpenMP` [9]. We use the Python library `matplotlib` [10] to produce all the plots, `seaborn` [11] to set the theme in the figures. We also use a linear regression method and the normal distribution method from the Python library `SciPy`. To optimize our implementation, we used a profiling tool `Score-P` [12].

III. RESULTS

A. Burn-in time

We started with a lattice size $L = 20$ and considered the temperatures $T_1 = 1.0J/k_B$, and $T_2 = 2.4J/k_B$, where T_2 is close to the analytical critical temperature given by Equation (17).

To determine the burn-in time, we used the numerical estimates of energy per spin for T_1 in Figure 3, and T_2 in Figure 5. We also considered the estimates of magnetization per spin for T_1 in Figure 2, and for T_2 in Figure 5.

The lattice was initialized in an ordered and an unordered state, for both temperatures. We observed no change in expectation value of energy or magnetization for T_1, when we initialized the lattice in an ordered state. As for the unordered initialized lattice, we first observed a change in expectation values, and a stabilization around 5000 Monte Carlo cycles. The expected energy per spin is $\langle\epsilon\rangle \approx -2$ and the expected magnetization per spin is $\langle|m|\rangle \approx 1$. For T_2 we observed a change in expectation values for both the ordered and the unordered lattice. For T_2 we observe an increase in expected energy per spin $\langle\epsilon\rangle \approx -1.25$, and a decrease in expected magnetization per spin $\langle|m|\rangle \approx 0.47$.

[1] Technical specifications for Fox can be found at https://www.uio.no/english/services/it/research/platforms/edu-research/help/fox/system-overview.md

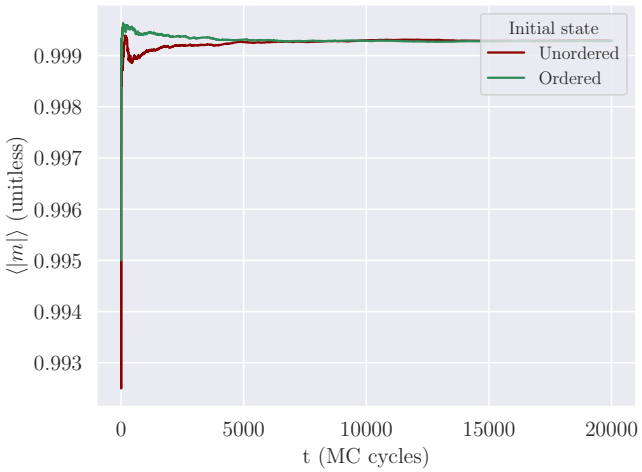

FIG. 2: Magnetization per spin $\langle|m|\rangle$ as a function of time t given by Monte Carlo cycles, for $T = 1.0J/k_B$

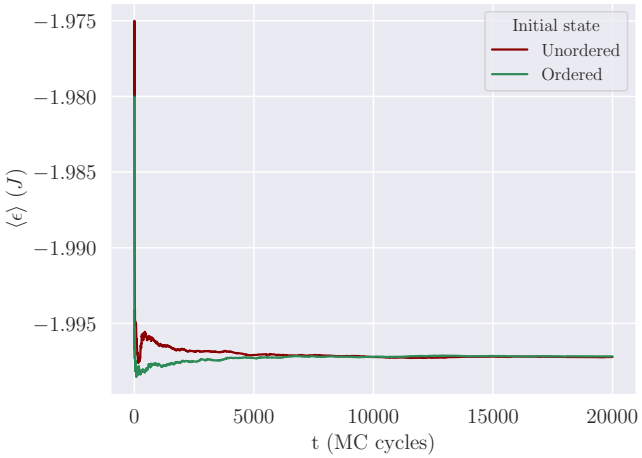

FIG. 3: Energy per spin $\langle\epsilon\rangle$ as a function of time t given by Monte Carlo cycles, for $T = 1.0J/k_B$

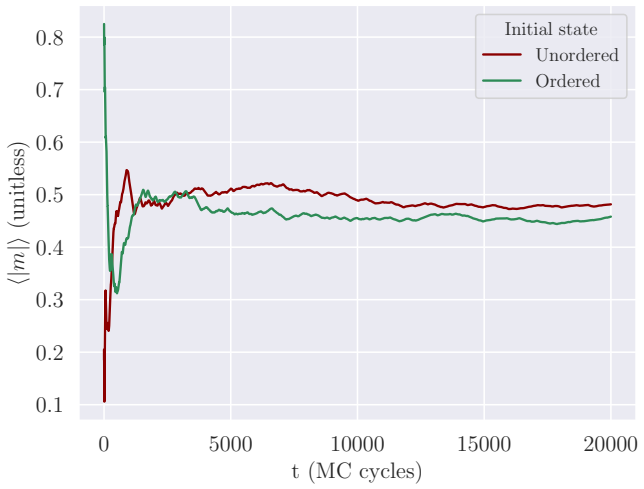

FIG. 4: Magnetization per spin $\langle|m|\rangle$ as a function of time t given by Monte Carlo cycles, for $T = 2.4J/k_B$

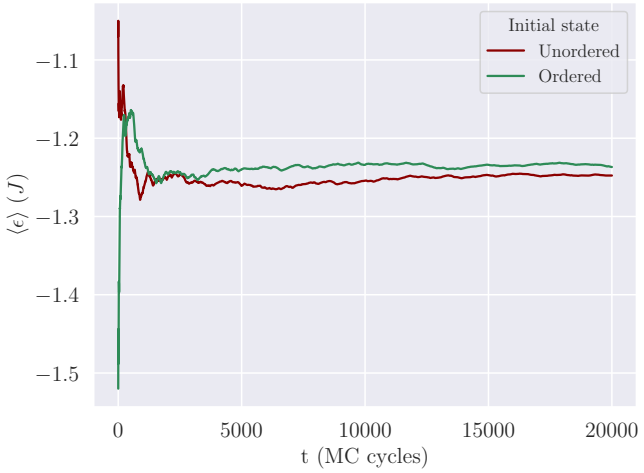

FIG. 5: Energy per spin $\langle\epsilon\rangle$ as a function of time t given by Monte Carlo cycles, for $T = 2.4J/k_B$

B. Probability distribution

We used the estimated burn-in time of 5000 Monte Carlo cycles as starting time, and generated samples. To visualize the distribution of energy per spin ϵ, we used histograms with a bin size 0.02. In Figure 6 we show the distribution for T_1. Where the resulting expectation value of energy per spin is $\langle\epsilon\rangle = -1.9972$, with a low variance of $\mathrm{Var}(\epsilon) = 0.0001$.

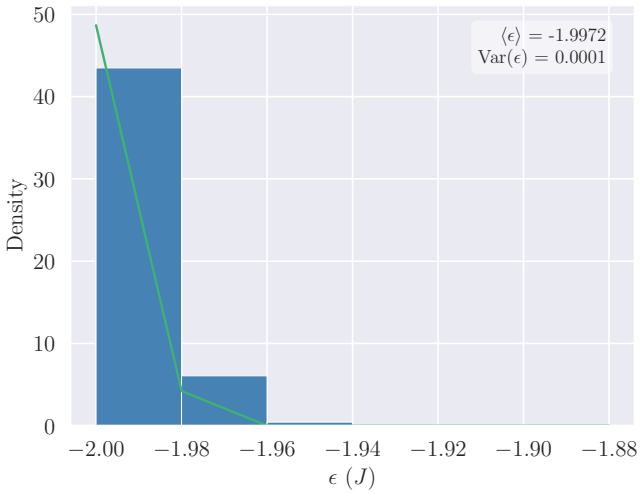

FIG. 6: Distribution of values of energy per spin, when temperature is $T = 1.0J/k_B$. The green line shows the normal curve $\mathcal{N}(\langle\epsilon\rangle, \mathrm{Var}(\epsilon))$.

In Figure 7, for T_2, the samples of energy per spin is centered around the expectation value $\langle\epsilon\rangle = -1.2367$.

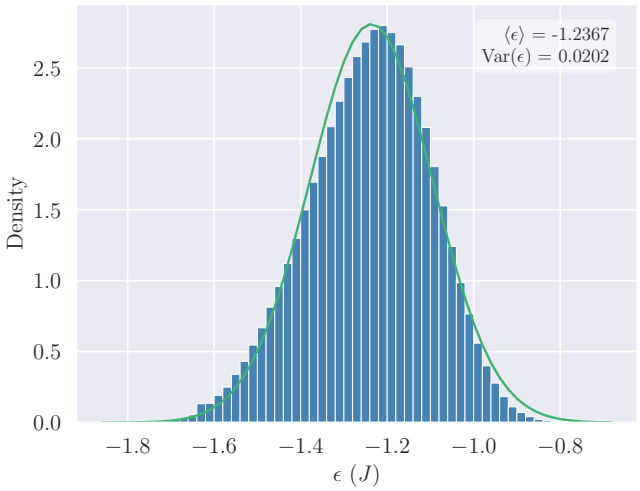

FIG. 7: Distribution of values of energy per spin, when temperature is $T = 2.4J/k_B$. The green line shows the normal curve $\mathcal{N}(\langle\epsilon\rangle, \mathrm{Var}(\epsilon))$.

However, we observed a higher variance of $\mathrm{Var}(\epsilon) = 0.0202$. When the temperature increased, the system moved from an ordered to an unordered state. The change in system state, or phase transition, indicates the temperature is close to a critical point.

C. Phase transition

We continued investigating the behavior of the system around the critical temperature. First, we generated 10

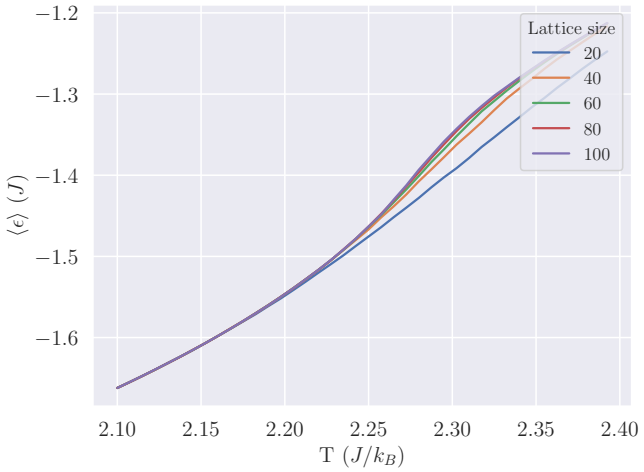

FIG. 8: Expected energy per spin $\langle\epsilon\rangle$ for temperatures $T \in [2.1, 2.4]$, and 10^7 MC cycles.

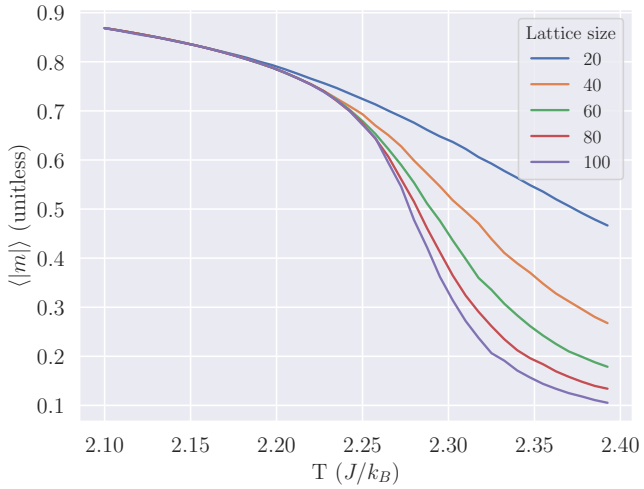

FIG. 9: Expected magnetization per spin $\langle|m|\rangle$ for temperatures $T \in [2.1, 2.4]$, and 10^7 MC cycles.

million samples of spin configurations, per temperature, for lattices of size $L \in \{20, 40, 60, 80, 100\}$, and temperatures $T \in [2.1, 2.4]$. We divided the temperature range into 40 steps, with an equal step size of 0.0075. The samples were generated in parallel, where the program allocated 4 sequential temperatures to 10 MPI processes. Each process was set to spawn 10 threads, resulting in a total of 100 threads working in parallel. We include results for 1 million MC cycles in Appendix F

To evaluate the performance of the parallelization, we used a profiler. The assessment output can be found in Appendix F in Figure 18. The assessment shows a lower score for the MPI load balance, compared to the OpenMP load balance. The master process gatheres all the data using blocking communication, resulting in the other processes waiting. This results in one process, the master, having to work more. The OpenMP load balance score is very good, suggesting that the threads are not left idle for long time periods.

In Figure 8, for the larger lattices we observe a sharper increase in $\langle\epsilon\rangle$ in the temperature range $T \in [2.25, 2.35]$. We observe a decrease in $\langle|m|\rangle$ for the same temperature range in Figure 9, suggesting that the system moves from an ordered magnetized state to a state of no net magnetization. The system energy increases, however, there is a loss of magnetization close to the critical temperature.

In Figure 10, we observe an increase in heat capacity in the temperature range $T \in [2.25, 2.35]$. In addition, we observe a sharper peak value of heat capacity when the lattice size increase.

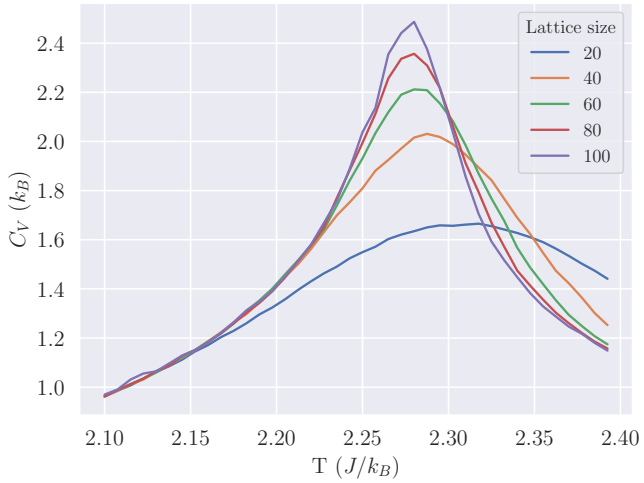

FIG. 10: Heat capacity C_V for temperatures $T \in [2.1, 2.4]$, and 10^7 MC cycles.

The magnetic susceptibility in Figure 11, shows the sharp peak in the same temperature range as that of the heat capacity. Since the shape of the curve for both heat capacity and the magnetic susceptibility become sharper when we increase lattice size, we are moving closer to the critical temperature.

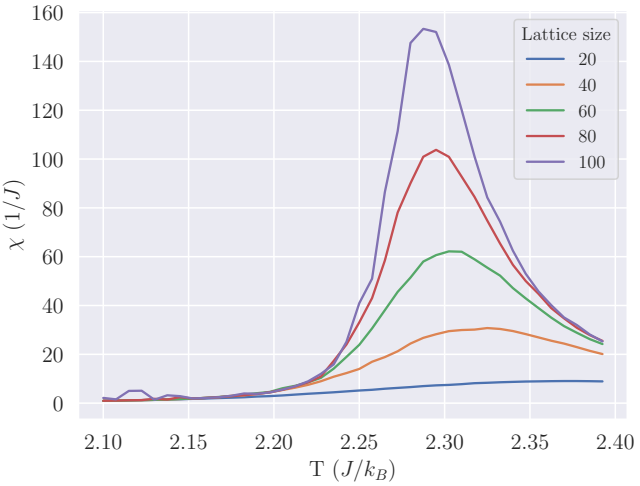

FIG. 11: Magnetic susceptibility χ for temperatures $T \in [2.1, 2.4]$, and 10^7 MC cycles.

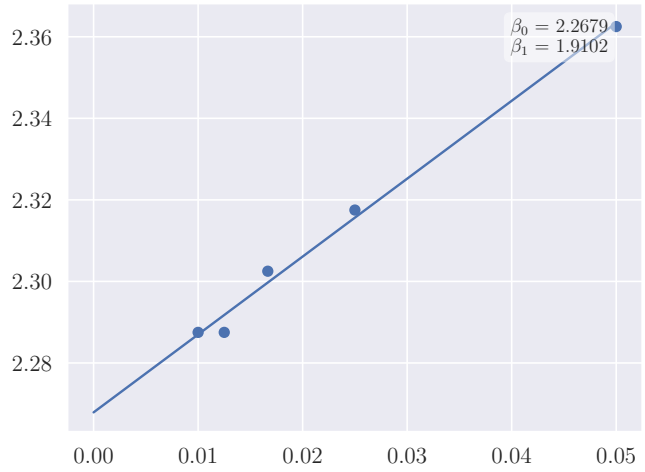

FIG. 12: Linear regression, where β_0 is the intercept approximating $T_c(L = \infty)$, and β_1 is the slope.

D. Critical temperature

Based on the heat capacity (Figure 10) and susceptibility (Figure 11), we estimated the critical temperatures of lattices of size $L \in \{20, 40, 60, 80, 100\}$ found in Table III.

L	$T_c(L)$
20	$2.37 J/k_B$
40	$2.325 J/k_B$
60	$2.3025 J/k_B$
80	$2.295 J/k_B$
100	$2.2875 J/k_B$

TABLE III: Estimated critical temperatures for lattices $L \times L$, where L denote the lattice size.

We used the critical temperatures of finite lattices and the scaling relation in Equation (16), Section II C, to estimate the critical temperature of a lattice of infinite size. In Figure 12, we plot the critical temperatures $T_c(L)$ of the inverse lattice size $1/L$. When the lattice size increase toward infinity, $1/L$ approaches zero.

We used linear regression to find the intercept β_0, which gives us an estimated value of the critical temperature for a lattice of infinite size. The estimated critical temperature is $T_c^*(L = \infty) \approx 2.2693 J/k_B$. We also compared the estimate with the analytical solution, the relative error of our estimate is

$$\text{Relative error} = \frac{T_c^* - T_c}{T_c} \approx 5.05405 \cdot 10^{-5} J/k_B$$

IV. CONCLUSION

We studied the ferromagnetic behavior of the Ising model, and observed a phase transition at temperatures close to the critical temperature. We used a Markov chain Monte Carlo sampling method to generate spin configurations, while utilizing parallel programming techniques. When increasing number of processes, and number of threads we observed a speed-up in runtime.

We initialized the lattices using both ordered and unordered spin configuration, and started sampling after the system reached an equilibrium. The number of Monte Carlo cycles necessary to reach a system equilibrium, referred to as burn-in time, was estimated to be 5000 cycles. We found that excluding the samples generated during the burn-in time, improves the estimated expectation value of energy and magnetization, in addition to the heat capacity and susceptibility, when samples are sparse. However, when we increase number of samples, excluding the burn-in samples does not affect the estimated values.

Continuing, we used the generated samples to compute energy per spin $\langle \epsilon \rangle$, magnetization per spin $\langle |m| \rangle$, heat capacity C_V, and χ. In addition, we estimated the probability distribution for temperatures $T_1 = 1.0 J/k_B$, and $T_2 = 2.4 J/k_B$. We found that for T_1 the expected mean energy per spin is $\langle \epsilon \rangle \approx -1.9972 J$, with a variance

$\mathrm{Var}(\epsilon) = 0.0001$. And for T_2, the mean energy per spin is $\langle\epsilon\rangle \approx -1.2367J$, with a variance $\mathrm{Var}(\epsilon) = 0.0202$.

We estimated the expected energy and magnetization per spin, in addition to the heat capacity and susceptibility for lattices of size $L = 20, 40, 60, 80, 100$. We observed a phase transition in the temperature range $T \in [2.1, 2.4]J/k_B$. Using the values from the finite lattices, we approximated the critical temperature of a lattice of infinite size. Using linear regression, we numerically estimated $T_c^*(L = \infty) \approx 2.2693J/k_B$ which is close to the analytical solution $T_c(L = \infty) \approx 2.269J/k_B$ Lars Onsager found in 1944.

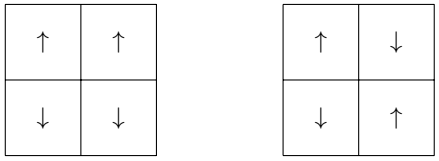

(a) (b)

FIG. 13: Possible spin configurations for two spins up.

Appendix A: Total energy

When two spins have the orientation up, the total magnetization is zero. However, the total energy of the system have two possible values, due to the location of the spin up as visualized in Figure 13.

Appendix B: Partition function

Using the values estimated for the 2×2 case, found in I, we find the partition function

$$\begin{aligned} Z &= 1 \cdot e^{-\beta(-8J)} + 4 \cdot e^{-\beta(0)} + 4 \cdot e^{-\beta(0)} \\ &\quad + 2 \cdot e^{-\beta(8J)} + 4 \cdot e^{-\beta(0)} 1 \cdot e^{-\beta(-8J)} \\ &= 2e^{8\beta J} + 2e^{-8\beta J} + 12. \end{aligned}$$

We rewrite the expression using the identity

$$\cosh(8\beta J) = 1/2\big(e^{8\beta J} + e^{-8\beta J}\big)$$

and find

$$z = 4\cosh(8\beta J) + 12 \ .$$

Appendix C: Expectation values

For a linear function of a stochastic random variable X, with a known probability distribution, the expected value of x is given by

$$\langle aX + b \rangle = a \cdot \langle X \rangle + b \qquad [13, \text{p. } 131]$$

In our case the discrete random variable is the spin configuration, and we want to find the expected value of the function $E(\mathbf{s})$.

Both energy per spin and magnetization per spin are functions of $\mathbf{s}$. In addition, the number of spins is given as a constant for each lattice. We can use the expression for $\langle E \rangle$ and $\langle M \rangle$ to find the expectation values per spin.

For energy per spin

$$\begin{aligned} \langle \epsilon \rangle &= \sum_{i=1}^{N} \epsilon(s_i) p(s_i \mid T) \\ &= \sum_{i=1}^{N} \frac{E(\mathbf{s})}{N} p(s_i \mid T) \\ &= \frac{1}{N} \sum_{i=1}^{N} E(\mathbf{s}) p(s_i \mid T) \end{aligned}$$

The same applies to magnetization per spin

$$\langle |m| \rangle = \frac{1}{N} \sum_{i=1}^{N} |M(s_i)| p(s_i \mid T) \ .$$

Continuing with the expectation values for a 2×2 lattice, excluding the terms which result in zero, we get

$$\begin{aligned} \langle E \rangle &= (-8J) \cdot \frac{1}{Z} e^{8\beta J} + 2 \cdot (8J) \cdot \frac{1}{Z} e^{-8\beta J} \\ &\quad + (-8J) \cdot \frac{1}{Z} e^{8\beta J} \\ &= \frac{16J}{Z}\big(e^{-8\beta J} - e^{8\beta J}\big) \\ &= -\frac{32J \sinh(8\beta J)}{4(\cosh(8\beta J) + 3)} \\ &= -\frac{8J \sinh(8\beta J)}{\cosh(8\beta J) + 3} \ , \end{aligned}$$

and

$$\begin{aligned} \langle |M| \rangle &= 4 \cdot \frac{1}{Z} \cdot e^{8\beta J} + 4 \cdot 2 \cdot \frac{1}{Z} \cdot e^{0} \\ &\quad + 4 \cdot |-2| \cdot \frac{1}{Z} \cdot e^{0} + |-4| \cdot e^{8\beta J} \\ &= \frac{8e^{8\beta J} + 16}{Z} \\ &= \frac{4(2e^{8\beta J} + 4)}{4(\cosh(8\beta J) + 3)} \\ &= \frac{2(e^{8\beta J} + 2)}{\cosh(8\beta J) + 3} \ . \end{aligned}$$

The squared energy and magnetization functions are then

$$\begin{aligned} \langle E^2 \rangle &= (-8J)^2 \cdot \frac{1}{Z} e^{8\beta J} + 2 \cdot (8J)^2 \cdot \frac{1}{Z} e^{-8\beta J} \\ &\quad + (-8J)^2 \cdot \frac{1}{Z} e^{8\beta J} \\ &= \frac{128J^2}{Z}\big(e^{8\beta J} + e^{-8\beta J}\big) \\ &= \frac{128J^2 \cosh(8\beta J)}{4(\cosh(8\beta J) + 3)} \\ &= \frac{64J^2 \cosh(8\beta J)}{\cosh(8\beta J) + 3} \ , \end{aligned}$$

and

$$\begin{aligned}\langle M^2\rangle &= 4^2\cdot\frac{1}{Z}\cdot e^{8\beta J} + 4\cdot 2^2\cdot\frac{1}{Z}\cdot e^0 \\ &\quad + 4\cdot(-2)^2\cdot\frac{1}{Z}\cdot e^0 + (-4)^2\cdot e^{8\beta J} \\ &= \frac{32e^{8\beta J}+32}{Z} \\ &= \frac{4(8e^{8\beta J}+8)}{4(\cosh(8\beta J)+3)} \\ &= \frac{8e^{8\beta J}+8}{\cosh(8\beta J)+3}\ .\end{aligned}$$

The squared expectation value is given by

$$\begin{aligned}\langle E\rangle^2 &= \left(-\frac{8J\sinh(8\beta J)}{\cosh(8\beta J)+3}\right)^2 \\ &= \frac{64J^2\sinh^2(8\beta J)}{(\cosh(8\beta J)+3)^2}\ ,\end{aligned}$$

and

$$\begin{aligned}\langle |M|\rangle^2 &= \left(\frac{2(e^{8\beta J}+2)}{\cosh(8\beta J)+3}\right)^2 \\ &= \frac{4(e^{8\beta J}+2)^2}{(\cosh(8\beta J)+3)^2}\ .\end{aligned}$$

Appendix D: Heat capacity and magnetic susceptibility

To find the heat capacity in Eq. 14, we normalize to heat capacity per spin

$$\begin{aligned}\frac{C_V}{N} &= \frac{1}{N}\frac{1}{k_BT^2}(\mathbb{E}(E^2)-[\mathbb{E}(E)]^2) \\ &= \frac{1}{Nk_BT^2}\mathbb{V}(E)\ .\end{aligned}$$

Using Equation (15), we find the susceptibility per spin

$$\begin{aligned}\frac{\chi}{N} &= \frac{1}{N}\frac{1}{k_BT}(\mathbb{E}(M^2)-[\mathbb{E}(M)]^2) \\ &= \frac{1}{Nk_BT}\mathbb{V}(M)\ .\end{aligned}$$

We now have to find the variance of both total energy and total magnetizaation. We obtain this using the definition

$$\begin{aligned}\mathbb{V}(X) &= \sum_{x\in D}[(x-\mathbb{E}(x))^2\cdot p(x)] \qquad \text{[13, p. 132]} \\ &= \mathbb{E}(X^2)-[\mathbb{E}(X)]^2\ .\end{aligned}$$

The variance of the total energy is then given by

$$\begin{aligned}\mathbb{V}(E) &= \mathbb{E}(E^2)-[\mathbb{E}(E)]^2 \\ &= \frac{64J^2\cosh(8\beta J)}{\cosh(8\beta J)+3} - \frac{64J^2\sinh^2(8\beta J)}{(\cosh(8\beta J)+3)^2} \\ &= 64J^2\left(\frac{\cosh(8\beta J)}{\cosh(8\beta J)+3} - \frac{\sinh^2(8\beta J)}{(\cosh(8\beta J)+3)^2}\right) \\ &= 64J^2\left(\frac{(\cosh(8\beta J))\cdot(\cosh(8\beta J)+3)}{(\cosh(8\beta J)+3)^2}\right. \\ &\quad \left. - \frac{\sinh^2(8\beta J)}{(\cosh(8\beta J)+3)^2}\right) \\ &= 64J^2\left(\frac{\cosh^2(8\beta J)+3\cosh(8\beta J)-\sinh^2(8\beta J)}{(\cosh(8\beta J)+3)^2}\right) \\ &= 64J^2\left(\frac{3\cosh(8\beta J)+1}{(\cosh(8\beta J)+3)^2}\right)\ ,\end{aligned}$$

and the variance of the total magnetization is given by

$$\begin{aligned}\mathbb{V}(M) &= \mathbb{E}(M^2)-[\mathbb{E}(|M|)]^2 \\ &= \frac{8e^{8\beta J}+8}{\cosh(8\beta J)+3} - \frac{4(e^{8\beta J}+2)^2}{(\cosh(8\beta J)+3)^2} \\ &= \frac{(8(e^{8\beta J}+1))\cdot(\cosh(8\beta J)+3)-4(e^{8\beta J}+2)^2}{(\cosh(8\beta J)+3)^2} \\ &= \frac{4(e^{8\beta J}+1)\cdot(e^{8\beta J}+e^{-8\beta J})}{(\cosh(8\beta J)+3)^2} \\ &\quad + \frac{24(e^{8\beta J}+1)-4(e^{8\beta J}+1)^2}{(\cosh(8\beta J)+3)^2} \\ &= \frac{4(3e^{8\beta J}+e^{-8\beta J}+3)}{(\cosh(8\beta J)+3)^2}\ .\end{aligned}$$

We find the heat capacity

$$\frac{C_V}{N} = \frac{64J^2}{Nk_BT^2}\left(\frac{3\cosh(8\beta J)+1}{(\cosh(8\beta J)+3)^2}\right)\ ,$$

and susceptibility

$$\frac{\chi}{N} = \frac{4}{Nk_BT}\left(\frac{3e^{8\beta J}+e^{-8\beta J}+3}{(\cosh(8\beta J)+3)^2}\right)\ .$$

Appendix E: Change in total system energy

When we consider the change in energy after flipping a single spin, we evaluate $\Delta E = E_{\text{after}} - E_{\text{before}}$. We find

the 3^2 values as

$$\begin{aligned}
\Delta E &= -8J - (-8J) = 0 \\
\Delta E &= -8J - 0 = -8J \\
\Delta E &= -8J - 8J = -16J \\
\Delta E &= 0 - (-8J) = 8J \\
\Delta E &= 0 - 0 = 0 \\
\Delta E &= 0 - 8J = -8J \\
\Delta E &= 8J - (-8J) = 16J \\
\Delta E &= 8J - 0 = 8J \\
\Delta E &= 8J - 8J = 0,
\end{aligned}$$

where the five distinct values are $\Delta E = \{-16J, -8J, 0, 8J, 16J\}$.

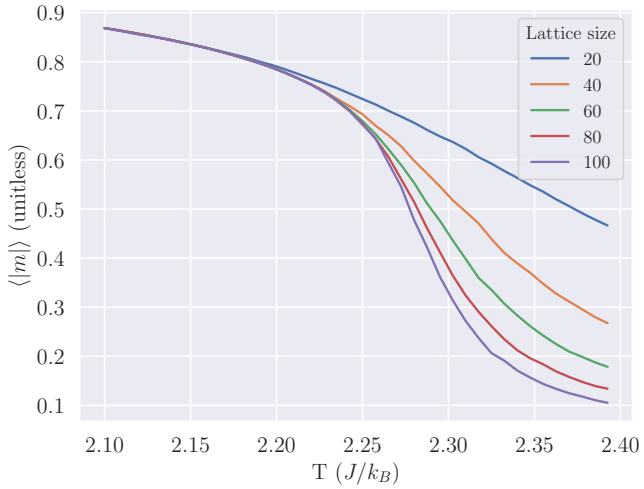

FIG. 15: Expected magnetization per spin $\langle |m| \rangle$ for temperatures $T \in [2.1, 2.4]$, and 10^6 MC cycles.

Appendix F: Additional results

We also did the phase transition experiment using 1 million MC cycles. In Figure 14 we show expected energy per spin, and in Figure 15 expected magnetization per spin.

In Figure 16 we show heat capacity, and in Figure 17 the magnetic susceptibility.

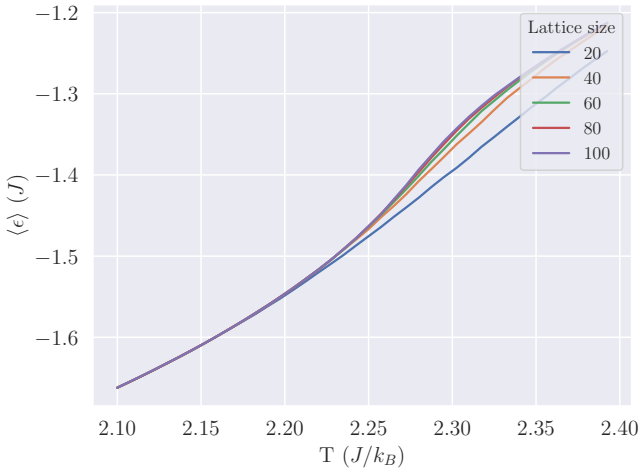

FIG. 14: Expected energy per spin $\langle \epsilon \rangle$ for temperatures $T \in [2.1, 2.4]$, and 10^6 MC cycles.

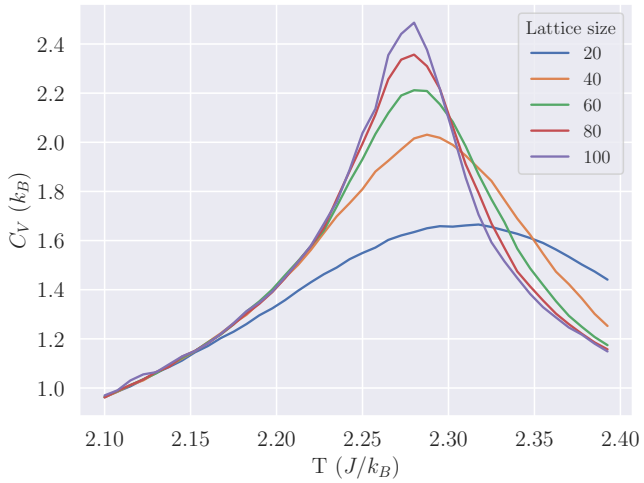

FIG. 16: Heat capacity C_V for temperatures $T \in [2.1, 2.4]$, and 10^6 MC cycles.

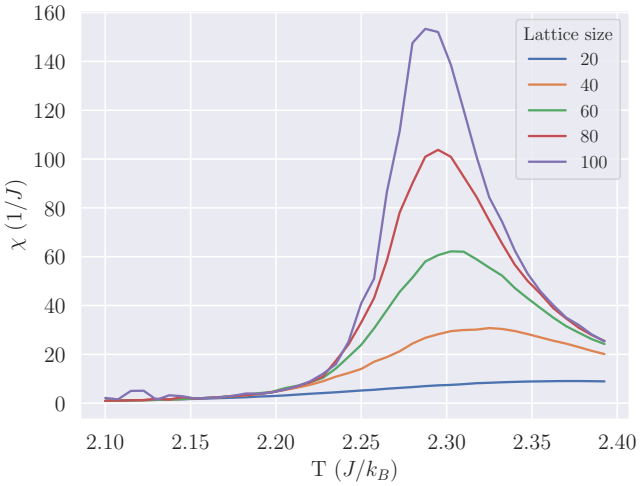

FIG. 17: Magnetic susceptibility χ for temperatures $T \in [2.1, 2.4]$, and 10^6 MC cycles.

Assessment of profiling using Score-P in Figure 18.

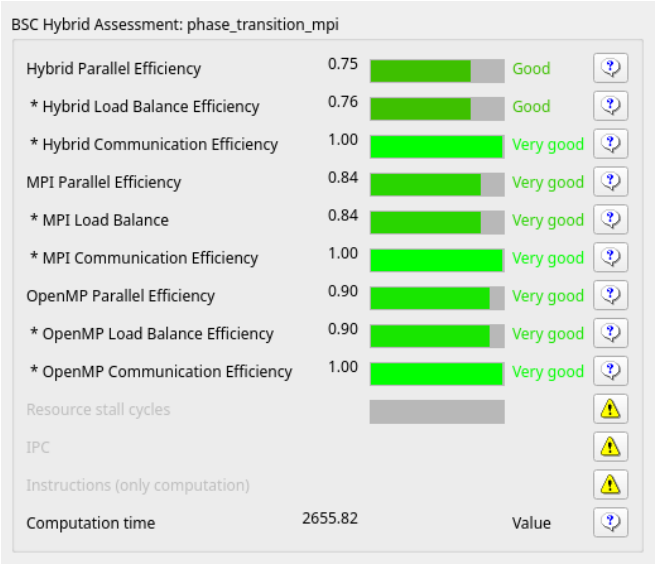

FIG. 18: Score-P assessment of parallel efficiency.

[1] Ismail-Beigi Research Group. Hard drives methods and materials, 2023. URL https://volga.eng.yale.edu/teaching-resources/hard-drives/methods-and-materials.

[2] The Editors of Encyclopaedia Britannica. ferromagnetism, 2023. URL https://www.britannica.com/science/ferromagnetism.

[3] Martin Niss. History of the lenz-ising model 1920-1950: From ferromagnetic to cooperative phenomena. *Archive for History of Exact Sciences*, 59(3), 2004.

[4] Gasper Tkacik, Elad Schneidman, Michal J. Berry II, and William Bialek. Ising models for network of real neurons. *arXiv*, 2008.

[5] Morten Hjorth-Jensen. Computational physics, lecture notes fall 2015. https://raw.githubusercontent.com/CompPhysics/ComputationalPhysics/master/doc/Lectures/lectures2015.pdf, 2015.

[6] Lars Onsager. Crystal statistics. i. a two-dimensional model with an order-disorder transition. *Physical review*, 65(3–4): 117–149, 1944.

[7] Shivam Agari. Monte carlo markov chain (mcmc), explained. URL https://towardsdatascience.com/monte-carlo-markov-chain-mcmc-explained-94e3a6c8de11.

[8] Edgar Gabriel, Graham E. Fagg, George Bosilca, Thara Angskun, Jack J. Dongarra, Jeffrey M. Squyres, Vishal Sahay, Prabhanjan Kambadur, Brian Barrett, Andrew Lumsdaine, Ralph H. Castain, David J. Daniel, Richard L. Graham, and Timothy S. Woodall. Open MPI: Goals, concept, and design of a next generation MPI implementation. In *Proceedings, 11th European PVM/MPI Users' Group Meeting*, pages 97–104, Budapest, Hungary, September 2004.

[9] OpenMP. Openmp application programming interface, 2018. URL https://www.openmp.org/wp-content/uploads/OpenMP-API-Specification-5.0.pdf.

[10] J. D. Hunter. Matplotlib: A 2d graphics environment. *Computing in Science & Engineering*, 9(3):90–95, 2007. doi: 10.1109/MCSE.2007.55.

[11] Michael L. Waskom. seaborn: statistical data visualization. *Journal of Open Source Software*, 6(60):3021, 2021. doi: 10.21105/joss.03021. URL https://doi.org/10.21105/joss.03021.

[12] Score-p: the scalable performance measurement infrastructure for parallel codes. URL https://perftools.pages.jsc.fz-juelich.de/cicd/scorep/tags/latest/html/. Tool suite for profiling and event tracing.

[13] Jay L. Devore and Kenneth N. Berk. *Modern Mathematical Statistics with Application*. Cham: Springer International Publishing AG, 3 edition, 2021.